Transpiration in the water-limited regime: soil-plant-atmosphere interactions

Alessandro Tarantino[1*] and *Eve* Roberts-Self[2]

[1]Department of Civil and Environmental Engineering, University of Strathclyde, G11XJ Glasgow, Scotland (UK)
[2]Department of Civil and Environmental Engineering, University of Strathclyde, G11XJ Glasgow, Scotland (UK)

Abstract. The use of vegetation to improve stability of natural and engineered slopes is an engineering Nature Based Solution. One effect of vegetation is to reinforce slopes 'hydrologically', i.e., by generating suction by the removal of soil water via transpiration. In turn, the depletion of soil water content reduces the hydraulic conductivity of the shallow layers of the soil, and this hinders rainwater infiltration during the wet period, possibly preserving suction in the deeper layers susceptible to failure. To improve upon this stabilising technique, it is key to develop transpiration models that account for the hydraulic characteristics of the soil and plant (below- and above-ground). In this way, modelling can guide the choice of the plant functional traits. This paper first discusses the conceptual and experimental limitations of common empirical evapotranspiration reduction functions (e.g. Feddes function) and then revisits the physically-based 'bottlenecks' generating the decline in evapotranspiration in the water-limited regime within the framework of the Soil-Plant-Atmosphere Continuum.

1 Introduction

Plants represent a potential Nature Based Solution [1-3] to improve the stability of natural and engineered slopes. Plants can reinforce slopes hydrologically by removing soil water via transpiration to generate stabilising suction. In turn, the depletion of soil water content reduces the hydraulic conductivity of the shallow layers of the soil, and this hinders rainwater infiltration during the wet period, possibly preserving suction in the deeper layers susceptible to failure. Plant-based hydrological reinforcement is key to reinforce slopes for the very frequent case of failure surfaces developing below the root zone (where root mechanical reinforcement plays no role).

Evapotranspiration occurs in two different regimes, 'energy-limited' and 'water-limited' respectively. Energy-limited (potential) evapotranspiration occurs when the soil-plant system can supply the water demanded by the atmosphere. It is controlled by the solar radiation (supplying the latent heat required to convert liquid into vapour water) and the near-surface vapour pressure, in turn controlled by the far-field water vapour pressure and near-field air turbulence.

When the degree of saturation and, hence, the hydraulic conductivity of the soil declines, the soil-plant system is not able to accommodate the evaporative demand of the atmosphere and the evapotranspiration reduces (water-limited regime). A very convenient and widely adopted empirical approach to model water uptake by vegetation in these two regimes is to multiply the potential evapotranspiration PET by a reduction factor assumed to be a function of soil suction in the root zone (e.g., Feddes function [4]). This approach is convenient in geotechnical numerical modelling because it only requires information about the suction in the root zone without the need to address the complex interaction between the soil, the plant, and the atmosphere. However, this simplicity is only apparent because the complexity of such an interaction is hidden in the 'empirical' choice of the parameters for the reduction function.

To improve upon vegetation-based hydrological stabilising techniques, it is vital to develop physically-based transpiration models that account for the hydraulic characteristics of the soil, the plant (below- and above-ground), and the atmosphere in order to guide the choice of suitable plant functional traits.

This paper discusses the conceptual and experimental limitations of common evapotranspiration reduction functions and revisits the plant science literature to identify the bottlenecks generating the decline in evapotranspiration in the water-limited regime within the framework of the Soil-Plant-Atmosphere Continuum (SPAC). This paves the way to the development of SPAC-based transpiration reduction functions.

2 Transpiration reduction function

2.1 Feddes formulation

A very common approach to model water uptake by vegetation macroscopically is to consider actual transpiration, AT, as the product of the potential (energy-

* Corresponding author: alessandro.tarantino@strath.ac.uk

limited) transpiration, *PT*, multiplied by a reduction factor, β, assumed to be a function of the suction in the root zone, s_{bulk}:

$$AT = PT \cdot \beta(s_{bulk}) \quad [1]$$

Under optimal soil water conditions, root water extraction rate is equal to the maximum transpiration rate, PT (β=1). Under non-optimal conditions, i.e., the soil is either too dry or too wet, transpiration is reduced by means of the factor β (β<1). Feddes et al. [4] assumes that the reduction factor is a function of soil suction in the root zone as presented in Fig. 1. The evapotranspiration is assumed to be equal to zero for suction lower than s_1, the 'anaerobiosis point', and above the wilting point s_4; the transpiration is maximum (β=1) between s_2 and s_3, with the latter corresponding to the suction in the soil above which plant transpiration starts to be limited. The threshold suction s_3 marks the transition from the energy-limited (potential) evapotranspiration to the water-limited evapotranspiration and is the most critical parameter of the Feddes function [5].

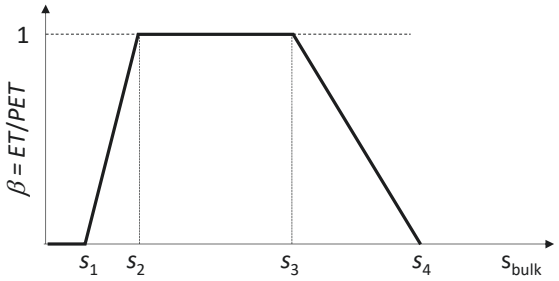

Fig. 1. Feddes reduction function [4]

The approach proposed by Feddes et al. [4] to model the reduction function is widely used in geotechnical applications [5-11]. This approach is convenient because it only requires information about the pore-water pressure in the root zone. Transpiration can be modelled via a suction-dependent sink term in the water flow equation.

The transition from the energy-limited (β=1) to the water-limited regime (β<1) and the rate at which transpiration decays in the water-limited regime is more complex and is associated with the interaction between the soil, the plant, and the atmosphere. The approach proposed by Feddes et al. [4] hides such an interaction by the choice of the Feddes parameters, which are often selected empirically.

The problem of the choice of the Feddes parameters is reflected in the very wide range of parameters adopted in the literature for s_3, as reported in Table 1. Feddes et al. [4] proposed s_3=-40 kPa, but a wide range of values for s_3 has been derived by Utset et al. [14] and Wesseling [15] depending on the nature of the crop and the potential transpiration rate. When the Feddes function is used in geotechnical applications, the parameter s_3 is generally borrowed from the agricultural literature. This approach may be questionable as the parameters derived for crop species and often loosely compacted organic agricultural soils may significantly differ from non-crop species in often densely-compacted soils that are typically encountered in geotechnical applications [16].

Table 1. Values of the Feddes parameters adopted in the literature (after [13])

			s_1 [kPa]	s_2 [kPa]	s_3 [kPa]	s_4 [kPa]
Feddes	[4]		-5	-5	-40	-1500
Agricultural crop models	[15]	Potatoes	1	2.5	32/60	1600
		Sugar beet	1	2.5	32/60	1600
		Wheat	0	0.1	50/90	1600
		Pasture	1	2.5	20/80	800
		Corn	1.5	3	32.5/60	800
	[14]	Potatoes	1	3.5	32/60	800
Geotechnical models	[6]		5	5	40	1500
	[5]		0	5	100/400	1500
	[9]		4.9	4.9	40	1500
	[8]		0	5	150	1500
	[7]		0	0	100	1500
	[11]		0	5	50	1500
	[16]		0.1	5	52/90	1500

2.2 Experimental transpiration reduction curves

The role played by the complex interactions between soil, plant, and atmosphere on the transpiration reduction function can be investigated by inspecting experimental datasets published in the geotechnical and plant science literature.

2.2.1 Effect of potential transpiration rate

Denmead and Shaw [17] investigated the effects of potential transpiration rate of corn plants in silty clay loams. Containers 450 mm diameter and 610 mm height were installed in the field and irrigation was periodically withheld to generate depletion of soil moisture. Potential transpiration rates varied during the course of the experiment and this allowed the determination of transpiration reduction curves at different potential transpiration rates as shown in Fig. 2.

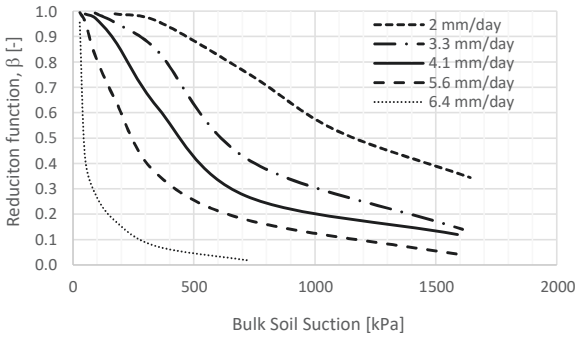

Fig. 2. Effect of potential transpiration rate on threshold suction s_3 and overall transpiration reduction function for corn plants and silty clay loams [17]

The threshold suction s_3 clearly increased by several hundreds of kPa as potential transpiration rate reduced from 6.4 mm/day to 2 mm/day. Fig. 2 highlights the role

played by the atmosphere (via the potential transpiration rate) in the transition from the energy-limited to the water-limited regime.

Similar results were obtained by Cai et al. [18] testing maize plants grown in two contrasting soil textures (sand and loam) and exposed to two consecutive Vapour Pressure Deficits (VPD) levels (1.8 and 2.8 kPa). Transpiration rate and soil water potential were measured during drying (Fig. 3). Again, the threshold suction s_3 clearly increased as VPD and, hence, potential transpiration rate reduced.

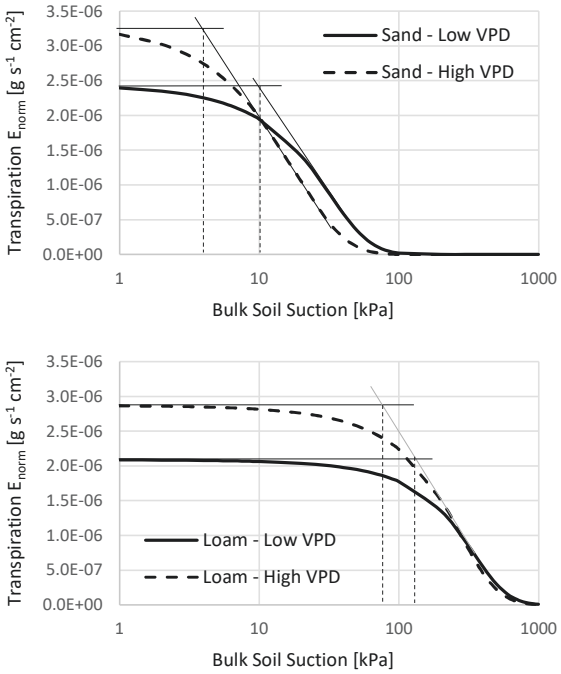

Fig. 3. Effect of potential transpiration rate on threshold suction, s_3, and overall transpiration reduction function for maize plants and sand/loam [18]

2.2.2 Effect of root length density

Ng et al. [19] investigated the effects of plant morphology on the response of the sink term to soil suction for *Schefflera heptaphylla*. Laboratory tests were conducted on 26 individual plants in five different groups of increasing height (S300T, S500T, S800T, L1000T, and L1200T). Transpiration data was presented in terms of Water Uptake Length Ability (WULA) [s^{-1}m^{-2}] versus bulk suction. WULA was defined as the ratio between Water Uptake Intensity (WUI), defined as the flow rate per unit volume [s^{-1}], and the Root Length Density (RLD), defined as total root length per unit volume (m^{-2}].

Data were re-converted in transpiration rate (flow rate per unit horizontal area [m/s]) by multiplying the WULA with the average Root Length Density and Root Depth as shown in Fig. 4.

It is observed again that the threshold suction s_3 decreases as transpiration rate increases (Fig. 5a). However, it is also observed that that the threshold suction, s_3, increases with the root length density (Fig. 5b). Therefore, root architecture also appears to control the transition from the energy-limited to the water-limited regime.

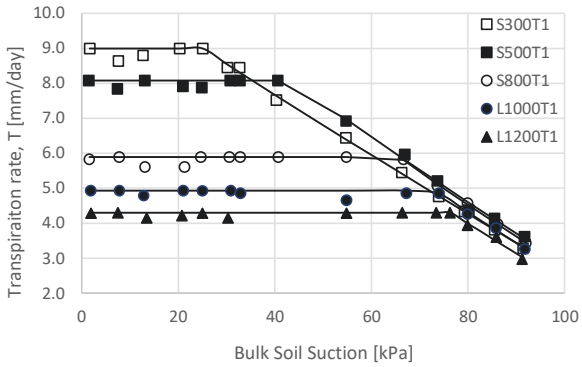

Fig. 4. Transpiration rates for *S. heptaphylla* trees in silty sand [19]

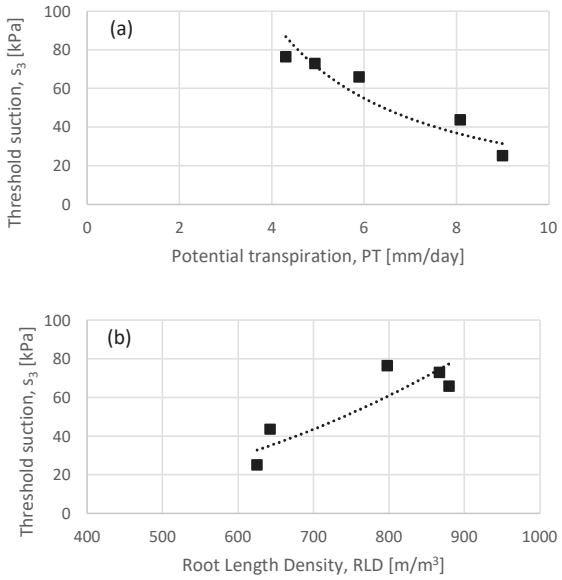

Fig. 5. Effect of potential transpiration rate and Root Length Density on threshold suction s_3 for *S. heptaphylla* tree in silty sand [19]

2.2.3 Effect of soil hydraulic properties

Data by Cai et al. [18] shows that the soil hydraulic properties also appear to control the transition from the energy-limited to the water-limited regime as shown in Fig. 6. In this case, the threshold suction s_3 appears to increase when moving from coarse-grained (sand) to fine-grained (loam) soil.

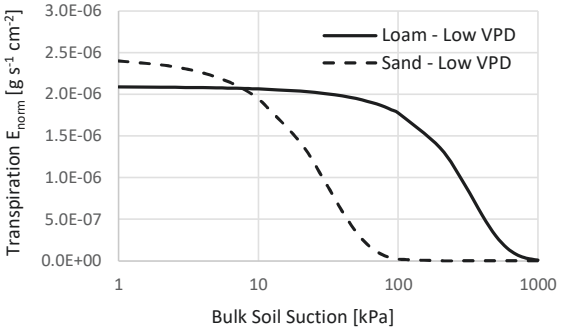

Fig. 6. Effect of soil type on transpiration reduction function for maize plants and sand/loam [18]

However, this is not always the case. Ni et al. [20] investigated the reduction in transpiration of one tree species (*S. heptaphylla*) transplanted in Completely Decomposed Granite (CDG, silty sand) and kaolin clay respectively. The comparison of the transpiration reduction curves for similar Leaf Area Index (LAI) and, hence, potential transpiration shows opposite trend. The threshold suction s_3 appears to decrease when moving from coarse-grained (silty sand, CDG) to fine-grained (kaolin clay) soil as shown in Fig. 7.

Although soil hydraulic properties clearly control the water-limited regime as shown in Fig. 6 and Fig. 7, their effect is not intuitive and requires further investigation.

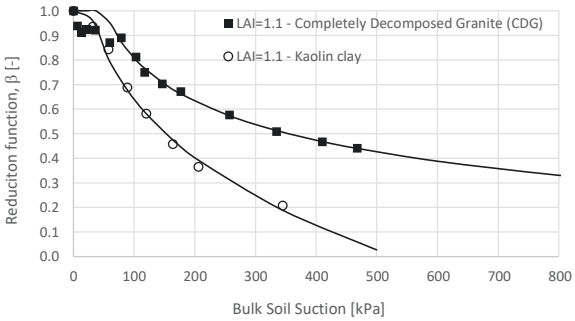

Fig. 7. Effect of soil type on transpiration reduction function for *S. heptaphylla* tree and silty sand/clay [20]

2.2.4 Non-linearity of transpiration reduction function

The water-limited branch of the transpiration reduction function is generally assumed to be linear between the threshold suction s_3 and the wilting suction s_4 (Fig. 1). However, experimental data often show that the water-limited branch of the reduction function is highly non-linear.

Non-linearity was observed by Garg et al. [16], measuring transpiration reduction of *Schefflera heptaphylla* with a range of Leaf Area Index (LAI) in clayey sand with gravel (Fig. 8a), and Dainese and Tarantino [13], measuring the transpiration reduction function of shrub willow (*Salix cinerea*) in silty sand (Fig. 8b). Non-linear water-limited branch of the transpiration reduction curve is also observed in Fig. 2 and Fig. 7.

2.2.5 Summary remarks

The datasets presented in this section underline the complex role played by the soil hydraulic properties, the root architecture, and the evaporative demand of the atmosphere in the reduction of transpiration. The interaction between these three components, i.e., soil, plant, and atmosphere, is therefore key to cast light on the mechanisms controlling the transpiration reduction function and to develop physically-based reduction functions.

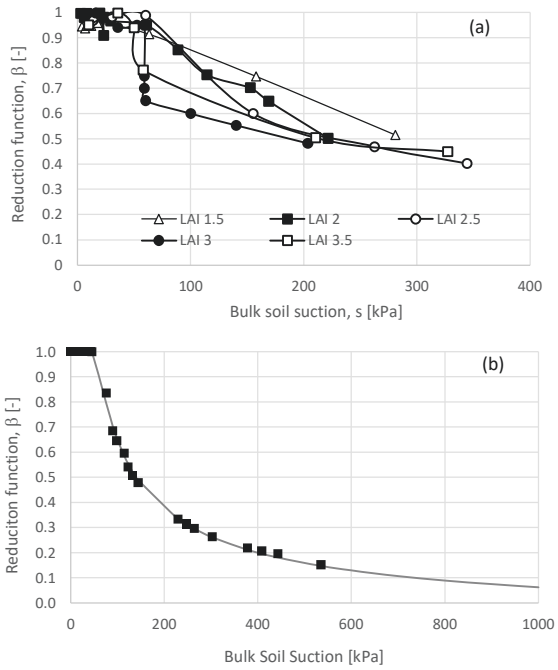

Fig. 8. Non-linearity of water-limited branch of the transpiration reduction function. (a) *S. heptaphylla* in clayey sand [16]. (b) *S. cinerea* in silty sand [13]

3 Soil-Plant-Atmosphere Continuum

Soil, plant, and atmosphere taken together form a physically integrated, dynamic system, which has been called the soil-plant-atmosphere continuum (SPAC) [21] (Fig. 9). Water flow takes place from regions of higher water potential in the bulk soil to regions of lower water potential in the atmosphere. This flow involves the movement of water in the bulk soil towards the roots, absorption into the roots, transport through the roots to the xylem and through the xylem to the leaves, evaporation in the intercellular air spaces of the leaves, vapour diffusion through stomatal openings to the boundary air layer in contact with the leaf surface, whence the vapour is finally transported to the external atmosphere. Each component of the SPAC system represents an in-series resistance to the water flow and its response is controlled by its hydraulic properties.

When water is available, evapotranspiration occurs at its maximum rate, and is controlled by the evaporative demand of the atmosphere (potential evapotranspiration). If potential evapotranspiration is increased, the hydraulic head differential between the bulk soil and the atmosphere must increase (Fig. 9). This is accompanied by an increase in suction in the bulk soil, soil-root interface, xylem and leaves and, in turn, this causes a decrease in hydraulic conductivity in each of these components. Eventually, a limit is approached beyond which one or more of the soil-plant components can no longer accommodate the potential evapotranspiration. Evapotranspiration is then controlled by the capacity of the soil-plant system to transmit water, regardless of the evaporative demand of the atmosphere. Each component of the SPAC is examined separately to explore the mechanisms that can turn each of these components into a ‘bottleneck’.

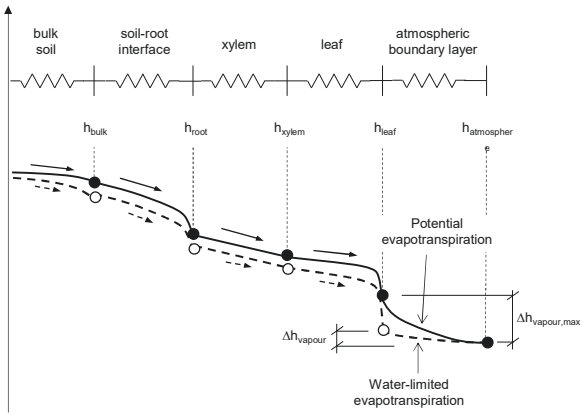

Fig. 9. Hydraulic resistances in the SPAC system

3.1 Bulk soil

3.1.1 Energy-limited and water-limited evaporation

The limiting condition in the bulk soil (the maximum water flux that can be accommodated by the bulk soil) is reached 'mathematically' when the suction at the ground level attains an infinite value. This concept is illustrated in Fig. 10. Let us consider the case of 1-D steady-state flow associated with a groundwater table at the bottom of a soil column and a prescribed pore-water pressure at the top boundary. If the pore-water pressure imposed at the top boundary is the hydrostatic pore-water pressure $u_{w,surface}$, the soil system returns zero flux at the top boundary. If the pore-water pressure imposed at the top boundary is lower that the hydrostatic pressure, the soil system returns an outward (upward) flux. If the pore-water pressure at the top boundary is further increased (in the limit to infinite), the outward flux increases but not indefinitely. A condition is reached whereby the outward flux levels off even if the pore-water pressure at the top boundary tends to $-\infty$.

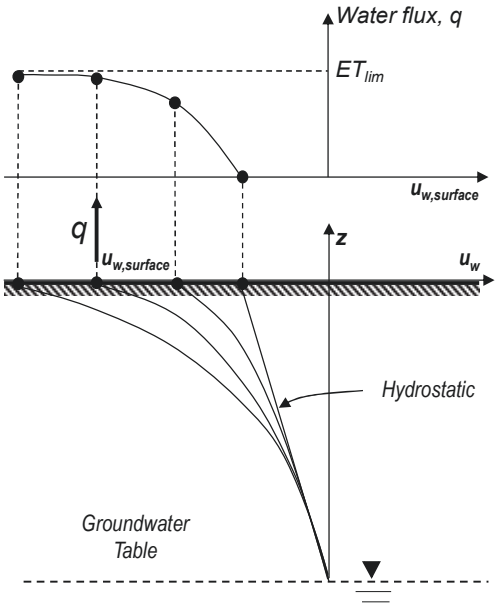

Fig. 10. The limited capacity of the soil hydraulic system to transfer water to the atmosphere.

The reason for this plateau is associated with the balance between the hydraulic gradient and the hydraulic conductivity. When the pore-water pressure at the top boundary goes to -∞, the hydraulic gradient i goes to infinite but the hydraulic conductivity k goes to zero. As a result, the flux $q = i \cdot k$ reduces to a finite value.

Fig. 10 also clarifies the difference between potential and water-limited evapotranspiration. Fig. 11a shows the case where the potential evapotranspiration, PET, is lower than the maximum water flux, ET_{lim}, that the soil system can transfer to the atmosphere. Under these conditions, the actual evapotranspiration equals the potential evapotranspiration ($AET=PET$).

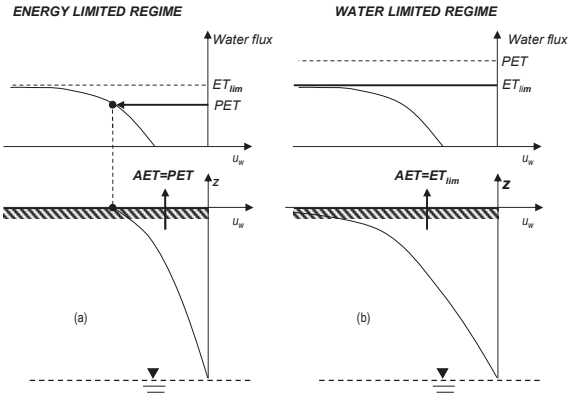

Fig. 11. The water-limited and the energy-limited regimes

Fig. 11b shows the case where the potential evapotranspiration, PET, is higher than the maximum water flux, ET_{lim}, that the soil system can transfer to the atmosphere. Under these conditions, the actual evapotranspiration equals the water limited evapotranspiration ($AET=ET_{lim}$).

3.1.2 Water-limited evaporation under steady-state conditions (bare soil)

Factors controlling the bulk soil flux limiting condition can be assessed by analysing the water flow equation including a water uptake term. For one-dimensional flow, Richards' equation can be written as:

$$\frac{\partial \theta}{\partial t} = \frac{\partial}{\partial z}\left[k(u_w)\frac{\partial}{\partial z}\left(\frac{u_w}{\gamma} + z\right)\right] - S(z) \qquad [2]$$

where θ is the volumetric water content, t [s] the time, z [m] the vertical coordinate increasing upward, u_w [kPa] the pore-water pressure, k [m s-1] the unsaturated hydraulic conductivity, and S [s-1] the sink term distributed in the root zone to simulate macroscopically the water uptake by the root system.

Analytical solutions of Eq. 2 for steady-state and transient flow are provided by Yuan and Lu [22] based on exponential functions for hydraulic conductivity k and volumetric water content θ:

$$k(u_w) = k_s e^{\alpha \frac{u_w}{\gamma_w}} \; ; \; \theta(u_w) = \theta_s e^{\alpha \frac{u_w}{\gamma_w}} \qquad [3]$$

Where u_w is the pore-water pressure, γ_w is the unit weight of water, k_s and θs the hydraulic conductivity and volumetric water content at saturation respectively, and

α is a soil parameter. Since the functions in Eq. 3 cannot reproduce accurately the hydraulic behaviour of soils, the analytical solutions have limited applicability to practical problems. Nonetheless, these analytical closed-form solutions allow understanding some key concepts about evaporation and transpiration and are explored in this section.

An example of the relatively poor capability of the exponential model given in Eq. 3 to fit experimental data is shown in Fig. 12. Hydraulic properties of pyroclastic soil [22] used in analytical examples and fitting using exponential and Brooks and Corey [24] models. The parameters of the exponential model are summarised in Table 2.

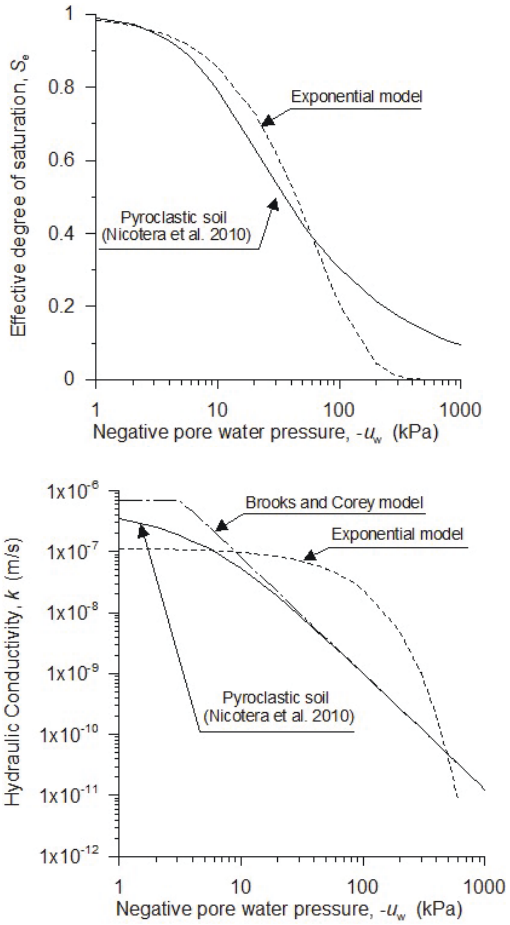

Fig. 12. Hydraulic properties of pyroclastic soil [22] used in analytical examples and fitting using exponential and Brooks and Corey [24] models

Table 2. Soil parameters used to derive analytical solutions.

θ_s	θ_r	α (1/m)	k_s (m/s)
0.659	0.164	0.157	1.13E-07

Steady-state solution for a bare soil column of thickness L, subjected to a water flux q_0 (positive upward) applied at the surface and zero pore-water pressure at the base of the column (Fig. 13), and an initial hydrostatic pore-water pressure profile is provided by Yuan and Lu [22]:

$$\frac{u_w}{\gamma_w} = \frac{1}{\alpha} ln\left[e^{-\alpha z} + \frac{q_0}{K_s}(e^{-\alpha z} - 1)\right] \quad [4]$$

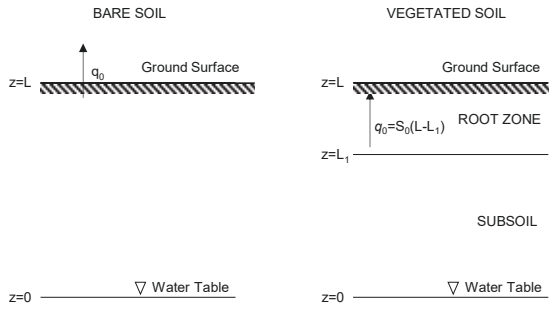

Fig. 13. Boundary conditions for analytical solutions of water flow for the case of bare and vegetated soils.

If this equation is re-written by extracting the water flux q_0 and the limit for $u_w(L)\rightarrow-\infty$ is considered, the water limiting evapotranspiration ET_{lim} can be derived for steady state conditions:

$$ET_{lim} = \lim_{u_w(L)\rightarrow-\infty} q_0 = \frac{k_s}{e^{\alpha L} - 1} \quad [5]$$

Eq. 5 shows that the transition from the energy-limited to the water limited regime is controlled by the characteristics of the hydraulic system as a whole, in this case the parameters k_s and α are associated with the hydraulic behaviour of the soil and the depth of the water table L. In turn, this highlights that the Feddes threshold suction s_3 depends at least on the soil hydraulic properties as clearly shown in Fig. 6 and Fig. 7.

The steady-state solution for a vegetated soil with constant extraction S_0 over the depth L-L_1 and overall outward flux q_0=S_0·(L-L_1) is also provided by Yuan and Lu [22]:

$$For\ 0 \le z \le L_1$$

$$u_w = \frac{\gamma_w}{\alpha} ln\left\{e^{-\alpha} + \frac{S_0}{K_s}(L - L_1)[e^{-\alpha z} - 1]\right\}$$

$$For\ L_1 \le z \le L \quad [6]$$

$$u_w = \frac{\gamma_w}{\alpha} ln\left\{\begin{array}{c} e^{-\alpha} + \frac{1}{K_s}\frac{S_0}{\alpha}[\alpha(L - L_1) + e^{\alpha L_1}]e^{-\alpha z} + \\ -\frac{1}{K_s}\frac{S_0}{\alpha}[\alpha(L - z) + 1] \end{array}\right\}$$

If this equation is re-written by extracting the water flux q_0 and the limit for $u_w(L)\rightarrow\infty$ is considered, the water limited evapotranspiration ET_{lim} can be derived for vegetated soil under steady state conditions:

$$ET_{lim} = \lim_{u_w(L)\rightarrow-\infty} q_0 = \alpha K_s \frac{(L - L_1)}{e^{\alpha L} - \alpha(L - L_1) - e^{\alpha L_1}} \quad [7]$$

Compared to Eq. 6, Eq. 7 [7] shows that root architecture (root depth L-L_1 in this case) also plays a role in controlling the water limited regime as shown in Fig. 5.

Fig. 14 shows the water-limited evapotranspiration from bare soil and vegetated soil with two different root

depths, δ=0.4m and δ=1.2m respectively. It can be observed that, at a given water table depth, roots can transfer a higher water flux to the atmosphere (via the plant) and this is due to the lower gradients generated in the soil when water extraction is distributed over a given depth (vegetated soil) rather than concentrated at the ground surface (bare soil).

Fig. 14 also highlights the differences in actual evapotranspiration between bare and vegetated soils for the case where evapotranspiration occurs in the water-limited regime. As an example, consider the case of water table depth L=6m and potential evapotranspiration PET = 8mm/day. Evapotranspiration occurs in the water-limited for both bare and vegetated soils. However, ET_{lim} is higher as root depth increases. In other words, the vegetation ensures a higher evapotranspiration in the water-limited regime.

On the other hand, if evaporation occurs in the potential (energy-limited) evapotranspiration, the same flux can be accommodated by both bare and vegetated soils regardless of root depth and there should not be a difference in evapotranspiration (if the potential evapotranspiration PET is the same for the bare and vegetated soils).

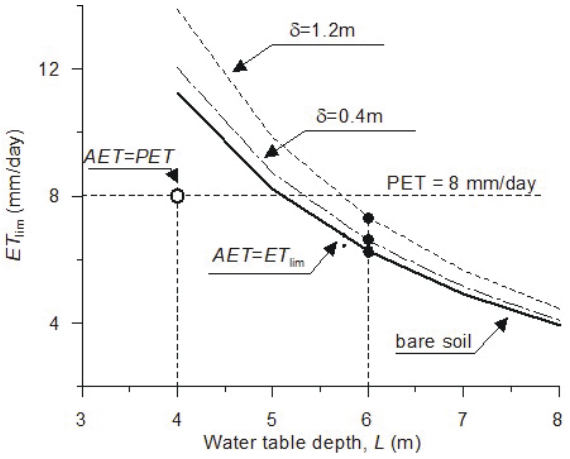

Fig. 14. Effect of mode of extraction on water-limited evapotranspiration under steady state conditions (δ=depth of root zone)

The curves in Fig. 14, although based on steady-state water flow and the assumption that potential evapotranspiration is the same for bare and vegetated soil, can provide a valuable conceptual tool to interpret field observations.

Fig. 15 shows measurements of matric suction at 1m depth for three covers, bare soil, soil vegetated with grass, and soil vegetated with mixed trees respectively [26]. Matric suction during the autumn-winter period is very similar for the three covers as if the three covers are subjected to the same evapotranspiration. It is likely that potential evapotranspiration is relatively low and, hence, lower than the water limited evapotranspiration for the three cases. Potential evapotranspiration can be accommodated by the three covers; actual evapotranspiration is therefore equal to the (similar) potential evapotranspiration for the three covers examined in Fig. 15.

On the other hand, matric suction during the spring-summer period is much higher for the case of mixed tree cover, as if the mixed tree cover is subjected to higher evapotranspiration. It is likely that potential evapotranspiration is relatively high and higher than the water limited evapotranspiration for the three cases. Potential evapotranspiration cannot be accommodated by the three covers and actual evapotranspiration is therefore equal to the water-limited evapotranspiration, which is higher for deeper root zone (mixed tree) compared to shallow root zone (grass) or bare soil as shown in Fig. 14.

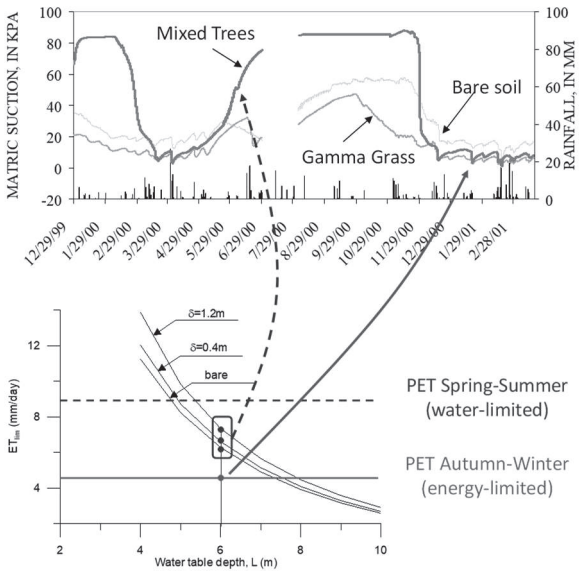

Fig. 15. Suction generated in bare and vegetated soil (after [26])

Fig. 14 is also consistent with empirical observation of evapotranspiration from different vegetated soils in Central Amazonia. Hodnett et al. [25] showed that, during wet season, evapotranspiration of a 'terra firme' type forest was very similar to that of pasture and the soil moisture under the two vegetation types showed little difference. This is consistent with Fig. 14. In the wet season, PET is low and is therefore likely to be lower than ET_{lim}. If this is the case, the soil can accommodate the same PET regardless of the root depth.

Hodnett et al. [25] observed that, in the dry season, the forest sustained a higher evapotranspiration rate compared to the pasture and the difference was attributed to the ability of the trees to access soil moisture from greater depth. This is again consistent with Fig. 14. In the dry season, PET is high and is therefore likely to be higher than ET_{lim}. If this is the case, the water-limited evapotranspiration ET_{lim} would be higher for the forest characterised by a deeper root zone.

3.1.3 Water-limited evaporation under transient conditions (bare soil)

It is instructive to consider the case of transient flow, even if limited to the case of a bare soil. The transient solution with constant surface flux q_1 (positive upward) and initial hydrostatic condition is provided by Pagano et al. [11]:

$$\frac{u_w}{\gamma_w} = \frac{1}{\alpha} ln\left\{e^{-\alpha z} - 8q_1 \frac{\alpha}{K_s} e^{\frac{\alpha(L-z)}{2}} \sum_{n=1}^{\infty} \frac{sin(\lambda_n L) sin(\lambda_n z)}{2\alpha + \alpha^2 L + 4L\lambda_n^2} \left[1 - e^{-D\left(\lambda_n^2 + \frac{\alpha^2}{4}\right)t}\right]\right\} \quad [8]$$

where λ_n is the n^{th} positive root of the equation:

$$sin(\lambda L) + (2\lambda/\alpha) cos(\lambda L) = 0 \quad [9]$$

If this equation is re-written by extracting the water flux q_1 and the limit for $u_w(L) \to \infty$ is considered, the water limiting evapotranspiration ET_{lim} can be derived for bare soil under transient conditions:

$$ET_{lim} = \lim_{u_w(L) \to -\infty} q_1 = \frac{\frac{K_s}{\alpha} exp(-\alpha L)}{8 \sum_{n=1}^{\infty} \frac{sin^2(\lambda_n L)}{2\alpha + \alpha^2 L + 4L\lambda_n^2} \left[1 - exp\left[-D\left(\lambda_n^2 + \frac{\alpha^2}{4}\right)t\right]\right]} \quad [10]$$

The effect of time on water-limited evaporation for the case of two water table depths is shown in Fig. 16 (soil parameters as per Table 2). It can be observed that, for prolonged evapotranspiration, the water limited evapotranspiration ET_{lim} reaches a plateau and this corresponds to the steady-state ET_{lim} shown in Fig. 14 and Eq. 5. However, for shorter evapotranspiration periods, where transient conditions occur, 'transient' ET_{lim} can be higher than the 'steady-state' value.

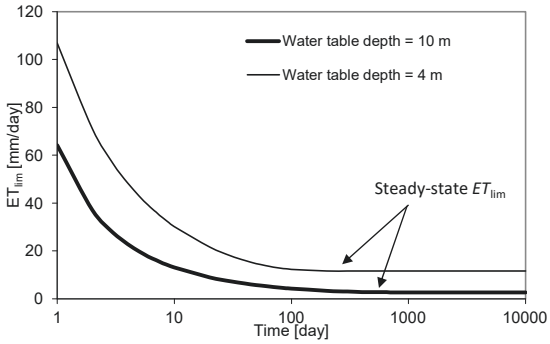

Fig. 16. Effect of time on water-limited evaporation from bare soil.

It is also worth noticing that the pore-water pressure at the ground surface, for the case where the flux applied at the boundary is a fraction F of the ET_{lim} ($q=F\ ET_{lim}$), is constant as shown by the equation below:

$$\left[\frac{u_w(L)}{\gamma_w}\right]_{q=F \cdot ET_{lim}} = \frac{1}{\alpha} ln[(1-F)] - L = constant \quad [11]$$

In other words, although the water-limiting conditions is achieved in theory for a pore-water pressure at the surface that tends to -∞, the limiting conditions achieved in practice for a finite constant value of pore-water pressure at the surface, which is a function of the soil hydraulic properties and the hydraulic boundary conditions. As shown later in the paper, this shows similarities with the mechanism occurring at the leaf controlling the transition from energy-limited to water-limited transpiration.

3.2 Soil-root interface

The most critical component of the SPAC is represented by the soil-root interface, which involves radial flow towards individual roots [27-29]. To isolate the soil and root characteristics that control the transition from energy-limited to water-limited transpiration, it is convenient to model the radial flow analytically.

The cylindrical single root model (Fig. 17) is used to analyse the soil-root system [30, 31]. Only a passive pathway is considered (water passes through the roots without the plant actively dedicating its resources into transporting water [31, 32]).

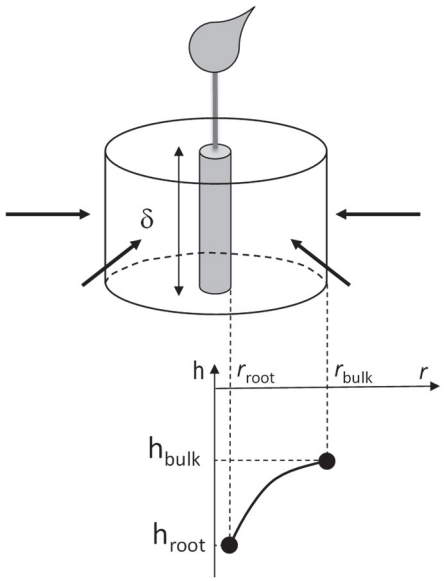

Fig. 17. Radial flow towards single root

The radial flow equation is written as follows:

$$\frac{\partial}{\partial r}\left[r \cdot k(h) \frac{\partial h}{\partial r}\right] = -\frac{\partial \theta}{\partial t} \quad [12]$$

where r is the radial coordinate in the reference system which has its origin at the centre of the root, k is the hydraulic conductivity, θ is the volumetric water content, and h is the pore-water pressure head. The latter is given by:

$$h = \frac{u_w}{\gamma_w} = -\frac{s}{\gamma_w} \quad [13]$$

where u_w is the pore-water pressure, s is the matric suction, and γ_w is the unit weight of water.

Under steady-state conditions, the water flow equation becomes:

$$\frac{\partial}{\partial r}\left[r \cdot k(h) \frac{\partial h}{\partial r}\right] = 0 \quad [14]$$

and considering the case where the hydraulic conductivity is modelled via an exponential function:

$$k = k_s \cdot \exp(\alpha h) \quad [15]$$

where k_{sat} is the hydraulic conductivity at zero pressure head and α is a soil parameter. Using the exponential hydraulic conductivity function, the solution of the steady-state equation can be derived as follows:

$$Q = \frac{2\pi\delta_{root} k_s [exp(\alpha h_{bulk}) - exp(\alpha h_{root})]}{\alpha \cdot ln\left(\frac{r_{bulk}}{r_{root}}\right)} \quad [16]$$

where h_{bulk} and h_{root} are the pressure head in the bulk soil and at the root respectively, δ_{root} is the length of the root segment, and Q is the flow rate through the single root. The flow rate through a single root is linked to the transpiration T as follows:

$$T = Q \cdot N \quad [17]$$

where N is the number of roots per unit horizontal area.

Let us consider the simplified root architecture in Fig. 18. The geometrical parameters characterising the radial flow domain, N, r_{bulk}, and δ_{root}, can be expressed in terms of the Root Length Density (RLD), and the root zone depth, $\delta_{root\text{-}zone}$, as follows:

$$\delta_{root} = \delta_{root\_zone} \quad [18]$$

$$N = RLD \quad [19]$$

$$r_{bulk} = 1/\sqrt{\pi RLD} \quad [20]$$

Note that Eq. 20 is an agreement with Duursma et al. [34].

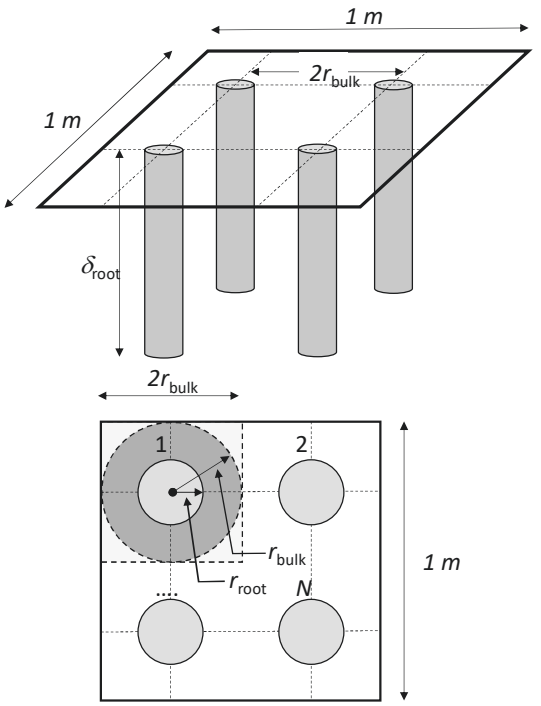

Fig. 18. Root architecture

By combining Eqs. 16 to 20 and considering Eq. 13, the suction at the root, s_{root}, can be expressed as a function of the suction in the bulk soil, s_{bulk}:

$$s_{root} = -\frac{\gamma_w}{\alpha} \ln\left[exp\left(-\alpha \frac{s_{bulk}}{\gamma_w}\right) - \frac{T}{RLD} \frac{1}{2\pi\delta_{root\_zone} k_s} \alpha \cdot ln\left(\frac{1/\sqrt{\pi RLD}}{r_{root}}\right)\right] \quad [21]$$

Eq. 21 is plotted in Fig. 19 and shows that s_{root} increases exponentially with s_{bulk} (root architecture parameters used in the simulation are reported in Table 3). This analysis is consistent with experimental findings by Caron et al. [35] and Cai et al. [36].

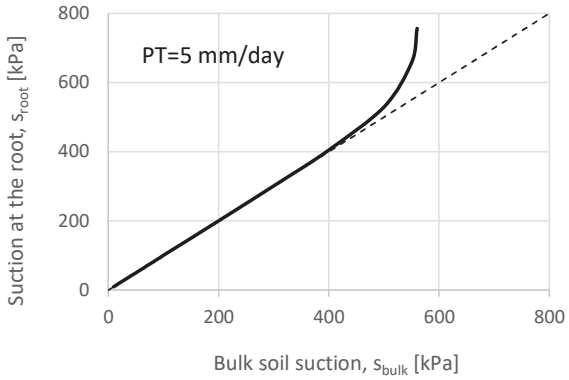

Fig. 19. Suction at the root versus suction in the bulk soil

Table 3. Root architecture parameters used to derive analytical solutions

$\delta_{root\ zone}$ [m]	RLD [m^{-2}]	r_{root} (m)
0.4	800	0.0005

The curve in Fig. 19 helps explain the transition from the energy-limited to the water-limited regime. When the soil is 'wet' and transpiration occurs in the energy-limited regime, s_{bulk} is relatively low and s_{root} required to accommodate the potential transpiration is also relatively low, compatible with the suction that can be sustained by the xylem.

When the soil dries out, s_{bulk} increases and s_{root} increases more than linearly to accommodate the potential transpiration. Eventually, a condition is reached where s_{root} attains a limiting value of suction that can be sustained by the xylem, $s_{root,max}$ (the existence of a critical suction value in the plant xylem/leaf is discussed in the next section). As s_{root} cannot increase anymore, the flow rate towards the roots declines and transpiration enters the water-limited regime.

The threshold suction s_3 marking the transition from the energy-limited to the water-limited regime can be derived analytically by considering that:

$$s_3 = s_{bulk} \ when \ s_{root} = s_{root,crit} \ \ and \ T = PT \quad [22]$$

where PT is the Potential Transpiration. The threshold suction s_3 is given by the following expression:

$$s_3 = \frac{\gamma_w}{\alpha} \cdot \quad [23]$$

$$\cdot \ln\left[\frac{1}{\underbrace{PT}_{(1)}\underbrace{\frac{\alpha}{2\pi k_s}}_{(2)}\underbrace{\frac{ln\left(\frac{1/\sqrt{\pi RLD}}{r_{root}}\right)}{RLD\cdot\delta_{root}}}_{(3)}+exp\left(-\frac{\alpha s_{root,crit}}{\gamma_w}\right)}\right]$$

Eq. 23 captures the effect of the evaporative demand of the atmosphere (Term *1*), soil hydraulic properties (Term *2*), and root architecture properties (Term *3*).

It is interesting to observe that Eq. 23captures the experimental transpiration reduction data presented in Section 2.2. The higher the potential transpiration, PT (Term *1* at the denominator of the right-hand side of Eq. 23), the lower is the threshold suction s_3 as observed in Fig. 2 and Fig. 3.

The higher the root length density, RLD, (term *3* at the denominator of the right-hand side of Eq. 23), the higher is the threshold suction s_3 as observed in Fig. 5.

The effect of soil hydraulic properties is more complex. The threshold suction is controlled by the saturated hydraulic conductivity k_{sat} and the 'shape' parameter α that indirectly affects the air-entry suction. These two parameters are competing and it is therefore difficult to anticipate whether s_3 increases or decrease when the soil texture changes from coarse-grained to fine-grained. This explains the contrasting results observed in Fig. 6 and Fig. 7.

3.3 Xylem

Soil water converges radially to the root and crosses the root cortex, reaching the xylem vessels, and moves upwards towards the leaves. The hydraulic resistance in the pathway from the root to the leaf is mainly associated with the hydraulic resistance of the root cortex, in turn associated with root diameter and cortex width [37]. Roose and Fowler [33] assumes that the cortex width is proportional to the root diameter; as a result, the root transmittance becomes independent of the root diameter.

The hydraulic conductivity (L_p) of the root system is in the order of 10^{-7} m s^{-1} MPa^{-1} for herbaceous plants and 10^{-8} m s^{-1} MPa^{-1} for woody plants [37, 38]. The transpiration rate accommodated by the xylem is proportional to the difference between the suction at the root, s_{root}, and the suction at the leaf, s_{leaf}:

$$T = N\,(2\,\pi\,r_{root}\cdot\delta_{root})\left[L_p\left(s_{leaf}-s_{root}\right)\right] \quad [24]$$

By using Eqs. 18 and 19, the suction differential is given by:

$$s_{leaf}-s_{root} = \frac{T}{RLD\left(2\,\pi\,r_{root}\cdot\delta_{root\_zone}\right)L_p} \quad [25]$$

As an example, this suction differential is plotted in Fig. 20 for an herbaceous plant with the root architecture parameters given in Table 3. This difference may be small compared to the loss of suction along the radial flow towards the root. If this is the case, the suction at the root, s_{root}, is approximately equal to the suction at the leaf, s_{leaf}.

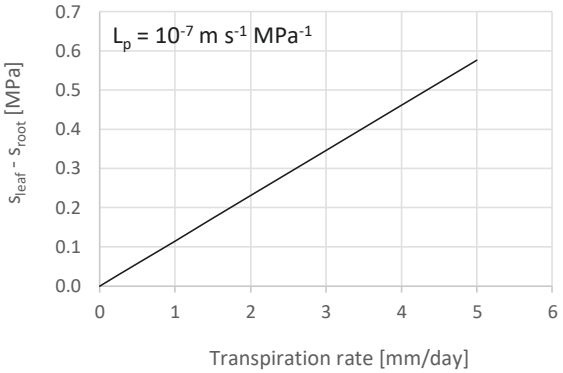

Fig. 20. Suction differential between suction at the root, s_{root}, and suction at the leaf, s_{leaf}, as a function of the transpiration rate

3.4 Leaf

Hochberg et al. [39] and Duursma et al. [34] assume that stomata in the water-limited regime are regulated to prevent the suction at the leaf, s_{leaf}, to raise above a critical value, $s_{leaf,crit}$. This assumption is based on the model of Sperry et al. [40] where the $s_{leaf,crit}$ is associated with turgor loss or catastrophic xylem cavitation (embolism). Different studies have linked stomatal closure with these physiological characteristics (e.g., [41]).

The existence of a critical value of the suction at the leaf, $s_{leaf,crit}$, which remains constant in the water limited-regime justifies the qualitative derivation of threshold suction s_3 in Eq. 23, where it was assumed that $s_{root,crit} \cong s_{leaf,crit}$.

4 Conclusions

This paper has discussed the problem of modelling plant transpiration in the energy-limited and water-limited regimes via transpiration reduction functions.

It first presented experimental evidence of reduction in transpiration rates as measured on different soil-plant systems. It has been shown that the transpiration reduction curve and the threshold suction s_3, marking the transition from energy-limited to water limited regime of transpiration, is controlled by the interaction of the evaporative demand of the atmosphere, the root architecture, and the soil hydraulic properties. The threshold suction s_3 decreases as the potential transpiration increases and increases as the root length density increases. The effect of soil hydraulic properties (soil texture) is more complex. The threshold suction s_3 may either increase or decrease when the soil texture changes from coarse-grained to fine-grained.

To elucidate these effects, the mechanisms of the reduction in transpiration have been analysed within the framework of the Soil-Plant-Atmosphere Continuum (SPAC). The flow of water occurs through four 'resistors' in series, i) bulk soil, ii) soil-root interface, iii) xylem, and iv) leaf.

Water flow in unsaturated 'bulk' soil has been analysed under 1D conditions by applying an outward water flux either concentrated at the ground surface (to

simulate evaporation from bare soil) or distributed within the top layer (to simulate water extraction by the roots). It has been shown that the water-limited evapotranspiration is controlled by the soil hydraulic system as a whole, including the soil hydraulic properties and the hydraulic boundary conditions (e.g., the position of the groundwater table). The threshold suction s_3 used to model the transition from energy-limited to water limited regime in unsaturated water flow modelling is therefore linked to the 'transmissivity' of the hydraulic system rather than being a property of the soil or the plant.

Radial flow towards a single root has been analysed to investigate the hydraulic processes occurring at the soil-root interface. By assuming that there exists a maximum suction that the root/xylem/leaf can sustain and that this critical suction is maintained constant by the plant in the water-limited regime, an analytical expression has been derived for the threshold suction s_3, which captures the complex interaction of the soil, plant and atmosphere and provides a simple framework to interpret experimental transpiration reduction data.

Finally, the existence of a critical value of the suction at the leaf, which remains constant in the water limited-regime when transpiration declines from its potential value, has been briefly discussed by reviewing plant science literature.

References

1. B. Kalsnes, V. Capobianco, Klima 2050 Report No 16 (2019)
2. L. Ruangpan, Z. Vojinovic, S. Di Sabatino, L. S. Leo, V. Capobianco, A, M. P. Oen, M. E. McClain, E. Lopez-Gunn, Nat. Hazards Earth Syst. Sci. **20**, 243-270 (2020)
3. T. de Jesús Arce-Mojica, U. Nehren, K. Sudmeier-Rieux, P. J. Miranda, D. Anhuf. Int. J. Disaster Risk Reduct. **41**, 101293 (2019)
4. R.A. Feddes, P.J. Kowalik, H. Zaradny. *Simulation of field water use and crop yield*. Pudoc, Wageningen. Simulation Monographs (1978).
5. V. Nyambayo, D.M. Potts, Computers and Geotechnics **37**, 175-186 (2010)
6. B. Indraratna, B. Fatahi, and H. Khabbaz. Proceedings of the Institution of Civil Engineers – Geotechnical Engineering, **159**, 77–90 (2006)
7. K.M. Briggs, J.A. Smethurst, W. Powrie, A.S. O'Brien. The influence of tree root water uptake on the long, Transportation Geotechnics, **9**, 31–48 (2016)
8. R. Greco, L. Comegna, E. Damiano, A. Guida, L. Olivares, L. Picarelli, Earth Syst. Sci., **17**, 4001–4013 (2013).
9. S. Hemmati, B.Gatmiri, Y.-J., Cui, M. Vincent, Journal of Multiscale Modelling, **2**, 163-184. (2010)
10. L. Pagano, A. Reder A, G. Rianna Effects of vegetation on hydrological response of silty volcanic covers, **56**, 1261-1277 (2018).
11. A. Tsiampousi, L. Zdravkovic, D.M. Potts Can. Geotech. J., **54**, 405–418 (2017).
12. H. Zhu, L. Zhang, Georisk: Assessment and Management of Risk for Engineered Systems and Geohazards (2019):
13. R. Dainese, A. Tarantino, Géotechnique, **71**, 441-454 (2021)
14. A. Utset, M. E. Ruiz, J. Garcia, R. A. Feddes, Potato Research, **43**(1), 19-29 (2000)
15. J.G. Wesseling. *Meerjarige simulatie van grondwaterstroming voor verschillende bodemprofielen, grondwatertrappen en gewassen met het model SWATRE*. DLO-Staring Centrum, Wageningen. Rapport / DLO-Staring Centrum no. 152 (1991)
16. A. Garg, A. K. Leung, and C. W. W. Ng., Catena, **135**, 78–82 (2015)
17. O. T. Denmead and R. H. Shaw, Agronomy Journal, 54, 385-390 (1962)
18. G. Cai, M. König, A. Carminati, M. Abdalla, M. Javaux, F. Wankmüller, and M.A. Ahmed, Plant Soil, https://doi.org/10.1007/s11104-022-05818-2 (2022).
19. C.W.W. Ng, Z.J. Wang, and J.J. Ni, Can. Geotech. J. **58**, 666–681 (2021)
20. J. J. Ni, C. W. W. Ng and H. W. Guo, *Effects of plant characteristics and soil type on transpiration reduction*, in Proceedings of the 7th International Conference on Unsaturated Soils, 3-8 August 2018, Hong-Kong (2018)
21. J.R. Philip, Ann. Rev. Plant Physiol., **17**, 245-268 (1966)
22. F. Yuan and Z. Lu, Vadose Zone Journal, **4**, 1210–1218 (2005)
23. M.V. Nicotera, R. Papa, G. Urciuoli, Geotechnical Testing Journal, **33**, 10.1520/GTJ102769 (2010)
24. R.H. Brooks and A.T. Corey, *Hydraulic properties of porous media*, Hydrology Paper No. 3, Colorado State University, Fort Collins, Colorado, 22–27 (1964)
25. M.G. Hodnett, L. Pimentel da Silva, H.R. da Rocha, and R. Cruz Senna., J. Hydrol., **170**, 233-254 (1995)
26. A. Simon and A.J.C. Collison, Earth Surf. Process. Landforms, **27**, 527–546 (2002)
27. A. Carminati, M. Javaux, Trends in Plant Science, **25**, 868-880 (2020)
28. W.R. Gardner, Soil Sci., **89**, 63–73 (1960)
29. E.I. Newman, J. Appl. Ecol. **6**, 1–12 (1969)
30. D.F. Whisler, A. Klute, R.J. Millington, Soil Science Society of America Journal, **34**, 382-387 (1970)
31. J.B. Passioura, Plant Physiology and Plant Molecular Biology, **39**, 245-65 (1988).
32. E., Steudle, C.A., Peterson, J. Exp. Bot. **49**, 775–788 (1998).
33. T. Roose, A.C. Fowler, Journal of Theoretical Biology, **228**, 155–171 (2004)
34. R. Duursma, P. Kolari. M. Perämäki, E. Nikinmaa, P. Hari, S. Delzon, D. Loustau, H. Ilviesnemi, J.

Pumpanen, A. Mäkelä, Tree Physiology **28**, 265–276 (2008).

35. J. Caron, H.L. Xu, P.Y. Bernier, I. Duchesne, P. Tardif, J. Amer. Soc. Hort. Sci., **123**, 931-936 (1998)
36. G. Cai M., A. Ahmed, M. Abdalla, and A. Carminati, Plant Cell Environ., **45**, 650–663 (2022)
37. M. Rieger and P. Litvin, Journal of Experimental Botany, **50**(331), 201–209 (1999).
38. E. Steudle, Plant and Soi, **226**, 45–56 (2000).
39. U. Hochberg, F.E. Rockwell, N. M. Holbrook, and H. Cochard, Trends in Plant Science, **23**, 112-120 (2018)
40. J.S. Sperry, F.R. Adler, G.S. Campbell, J.P. Comstock, Plant Cell Environ., **21**, 347–359 (1998)
41. Brodribb, T. N.M. Holbrook, E.J. Edwards, M.V. Gutiérrez, Plant Cell Environ., **26**, 443–450 (2003)